

Cite this: *RSC Adv.*, 2019, 9, 33222

NCPCDA: network consistency projection for circRNA–disease association prediction†

 Guanghui Li,^a Yingjie Yue,^b Cheng Liang,^c Qiu Xiao,^d Pingjian Ding^e
and Jiawei Luo^{*f}

A growing body of evidence indicates that circular RNAs (circRNAs) play a pivotal role in various biological processes and have a close association with the initiation and progression of diseases. Moreover, circRNAs are considered as promising biomarkers for disease diagnosis owing to their characteristics of conservation, stability and universality. Inferring disease–circRNA relationships will contribute to the understanding of disease pathology. However, it is costly and laborious to discover novel disease–circRNA interactions by wet-lab experiments, and few computational methods have been devoted to predicting potential circRNAs for diseases. Here, we advance a computational method (NCPCDA) to identify novel circRNA–disease associations based on network consistency projection. For starters, we make use of multi-view similarity data, including circRNA functional similarity, disease semantic similarity, and association profile similarity, to construct the integrated circRNA similarity and disease similarity. Then, we project circRNA space and disease space on the circRNA–disease interaction network, respectively. Finally, we can obtain the predicted circRNA–disease association score matrix by combining the above two space projection scores. Simulation results show that NCPCDA can efficiently infer disease–circRNA relationships with high accuracy, obtaining AUCs of 0.9541 and 0.9201 in leave-one-out cross validation and five-fold cross validation, respectively. Furthermore, case studies also suggest that NCPCDA is promising for discovering new disease–circRNA interactions. The NCPCDA dataset and code, as well as the detailed readme file for our code, can be downloaded from Github (<https://github.com/ghli16/NNPCPD>).

Received 7th August 2019
Accepted 3rd October 2019

DOI: 10.1039/c9ra06133a

rsc.li/rsc-advances

Introduction

Circular RNAs (circRNAs), a new category of noncoding endogenous RNA molecules, are generated by back-splicing of a single pre-mRNA and have a closed loop structure.¹ For many years, circRNAs were initially thought to be splicing errors.² Nonetheless, as high-throughput sequencing technology has developed, circRNAs have been shown to be widespread in various living organisms and garnered wide attention.^{3–6} Previous studies showed that circRNAs play a part in regulating the expression of genes as they function as microRNA sponges.⁷ For

instance, Cdr1as has been experimentally verified to work as a miR-7a sponge and to be involved in regulating the expression of SP1 and PARP.⁸ Importantly, the expression levels of circRNAs are generally tissue-specific and cell-type-specific.⁹ Consequently, circRNA misexpression can lead to abnormal physiological processes and account for the initiation and progression of most diseases.¹⁰

In recent years, an increasing number of circRNAs have been shown to function as tumor suppressors or oncogenes in various cancers.^{11,12} For example, Han *et al.* found that hsa_circ_0007874 inhibits the progression of hepatocellular carcinoma and promotes p21 expression by sponging miR-9.¹³ Likewise, hsa_circRNA_000479 serves as a sponge for miR-6809 and miR-4753 to modulate the expression of oncogene BCL11A, which can promote the proliferation of triple-negative breast cancer cells.¹⁴ CircCCDC66 is found to be correlated with poor prognosis of colorectal carcinoma and is up-regulated in various tumor tissues.¹⁵ High expression of circPVT1 in gastric cancer is closely related to a longer survival rate, suggesting that it is a prognostic marker for the disease.¹⁶ To summarise, both down-regulation and up-regulation of circRNAs in tumor cells shows that they may have the potential to be novel biomarkers and therapeutic targets. However, the current research on disease–circRNA relationships is highly dependent on

^aSchool of Information Engineering, East China Jiaotong University, Nanchang, 330013, China. E-mail: ghli16@hnu.edu.cn

^bSchool of Science, East China Jiaotong University, Nanchang, 330013, China. E-mail: yueyingjie001@163.com

^cCollege of Information Science and Engineering, Shandong Normal University, Jinan, 250000, China. E-mail: alcs417@hnu.edu.cn

^dCollege of Information Science and Engineering, Hunan Normal University, Changsha, 410081, China. E-mail: hnuyldf@hnu.edu.cn

^eSchool of Computer Science, University of South China, Hengyang, 421001, China. E-mail: dpjhnu@qq.com

^fCollege of Computer Science and Electronic Engineering, Hunan University, Changsha, 410082, China. E-mail: luojiawei@hnu.edu.cn

† Electronic supplementary information (ESI) available: One supplemental table is available as an excel file. See DOI: 10.1039/c9ra06133a



biological experiments, such as qRT-PCR and circRNAs chips, which are time-consuming and costly. In this case, only a limited number of relationships can be discovered.

Encouragingly, several manually curated databases of disease–circRNA interactions have become available, such as circRNADisease¹⁷ and CircR2Disease,¹⁸ which both collect experimentally verified associations by reviewing published literature. The establishment of disease–circRNA association datasets could provide an important foundation for predicting potential disease-related circRNAs using computational models. Recently, a lot of effort has gone into mining latent disease–circRNA pairs under the hypothesis that similar circRNAs are likely to have similar association profiles with the same disease. Lei *et al.*¹⁹ conducted a pioneer study in which they integrated a known disease–circRNA interaction network and multiple similarity networks for circRNAs and diseases into a heterogeneous network and presented a path-weighted method to excavate underlying disease-related circRNAs by counting the accumulative weights from paths with limited lengths in the constructed network. Likewise, Fan *et al.*²⁰ devised a KATZ-based model to quantify the association probability for each disease–circRNA pair by counting the number of walks with limited lengths between them on an established heterogeneous network, which was made up of a known disease–circRNA interaction matrix, a disease similarity matrix and a circRNA similarity matrix. Afterwards, Yan *et al.*²¹ designed a semi-supervised model based on Kronecker regularized least squares, which made predictions on a single circRNA–disease space by Kronecker product and capitalized on a preprocessing step to improve predictions for new circRNA nodes and disease nodes. Xiao *et al.*²² developed a novel model to recover the missing disease–circRNA interactions based on a low-rank approximation algorithm, which effectively combined manifold regularized constraints and produced reliable predictions. Recently, Wei *et al.*²³ constructed a circRNA–disease association probability matrix based on the neighbor interaction profiles. Specifically, this method prioritized disease-associated circRNAs by applying matrix factorization to the reconstructed association probability matrix. Zhang *et al.*²⁴ used a linear neighborhood to reconstruct the disease and circRNA similarity data, and then employed label propagation to measure the relevance between disease nodes and circRNA nodes. In addition, the advances in link prediction research in bioinformatics have also provided some valuable insights into the development of disease–circRNA interaction prediction (*e.g.*, synergistic drug combinations,²⁵ disease–lncRNA,^{26,27} disease–miRNA,^{28,29} and drug–target interaction prediction).³⁰ However, because of the incompleteness of the current datasets, it is still a challenge to achieve sufficiently accurate results for the prediction task.

In the present study, we advance a network consistency projection method (NCPCDA) for undiscovered circRNA–disease interaction predictions. In particular, NCPCDA implements a network consistency projection on the integrated circRNA similarity and disease similarity network to score circRNA–disease pairs. Simulation results under leave-one-out cross validation and five-fold cross validation evidently

demonstrate that NCPCDA performs better than previous models. Moreover, the case study carried out on lung cancer also suggests that our method is promising for identifying novel prognostic biomarkers.

Materials and methods

Human circRNA–disease associations

The known circRNA–disease association dataset was retrieved from the CircR2Disease database,¹⁸ which contains 739 experimentally confirmed interactions for 100 diseases and 661 circRNAs. After removing redundant entries from different literature and those relationships associated with mice and rats, we finally obtained a dataset consisting of 88 diseases, 585 circRNAs and 650 associations for humans. Formally, let $C = \{c_1, c_2, \dots, c_m\}$ and $D = \{d_1, d_2, \dots, d_n\}$ be the sets of m circRNAs and n diseases in the dataset, respectively. Thus, the binary matrix $Y \in R^{m \times n}$ of circRNA–disease interactions can be constructed, where $Y(i, j) = 1$ if circRNA c_i is connected to disease d_j , and 0 otherwise.

Disease semantic similarity

Inspired by the successful application of disease semantic similarity in prioritizing reliable disease-associated ncRNAs,^{31–36} we also capitalize on this similarity to enhance our predictions. As described in,³⁷ semantic similarities among diseases can be calculated according to their corresponding disease ontology,³⁸ which is organized as a directed acyclic graph. The disease ontology term for each disease in our analysis is retrieved from <http://disease-ontology.org/>. For two sets of disease ontology terms, we computed their similarity scores by using the “doSim” function in the DOSE software package.³⁹ For convenience, we use $SS \in R^{n \times n}$ to represent the semantic similarity matrix among n diseases.

CircRNA functional similarity

To quantify the functional similarity between circRNAs, the previous methods used for calculating the functional similarity between lncRNAs or miRNAs are extended.^{34,37} According to the previous work, evaluating the semantic similarity of two disease sets, which are linked with two circRNAs, can infer the function similarity of these two circRNAs. Particularly, we assumed that D_i and D_j were respectively the disease groups associated with circRNA c_i and circRNA c_j . Denote FS as the circRNA function similarity matrix, then the similarity between circRNA c_i and circRNA c_j can be computed by the following formulas:

$$FS(c_i, c_j) = \frac{\sum_{1 \leq p \leq |D_i|} S(d_p, D_j) + \sum_{1 \leq q \leq |D_j|} S(d_q, D_i)}{|D_i| + |D_j|} \quad (1)$$

$$S(d_p, D_j) = \max_{1 \leq t \leq |D_j|} (SS(d_p, d_t)) \quad (2)$$

where $S(d_p, D_j)$ is the similarity between disease d_p related to circRNA c_i and disease set D_j related to circRNA c_j .

As stated in the previous section, the disease semantic similarity can be calculated based on disease ontology terms.



However, we cannot obtain a disease ontology term for each disease. This means we are unable to measure the semantic similarities for those diseases without disease ontology terms. Therefore, association profile similarity is further introduced.

Association profile similarity for circRNAs and diseases

Association profile similarity is an effective topology similarity for diseases and circRNAs. For a specific circRNA c_i , the association profile of c_i is a binary vector, which is extracted from the i -th row vector of the circRNA–disease interaction matrix Y , i.e. $Y(i, :)$. Then, according to the Gaussian kernel function, we calculate the similarity between circRNA c_i and circRNA c_j as follows:

$$KC(c_i, c_j) = \exp(-\gamma_c \|Y(i, :) - Y(j, :)\|^2) \quad (3)$$

$$\gamma_c = 1 / \left(\frac{1}{m} \sum_{i=1}^m \|Y(i, :)\|^2 \right) \quad (4)$$

where γ_c , which is used to control the kernel bandwidth, is computed by normalizing the average number of diseases related to each circRNA.

Similarly, we also define disease association profile similarity as follows:

$$KD(d_i, d_j) = \exp(-\gamma_d \|Y(:, i) - Y(:, j)\|^2) \quad (5)$$

$$\gamma_d = 1 / \left(\frac{1}{n} \sum_{i=1}^n \|Y(:, i)\|^2 \right) \quad (6)$$

where $Y(:, i)$ indicates the interaction profile of disease d_i and γ_d is computed similarly to γ_c .

Integrated similarity for circRNAs and diseases

Considering that we cannot obtain circRNA functional similarity for all circRNAs in our dataset, we integrate functional similarity FS and association profile similarity KC to construct the circRNA similarity matrix CS. Particularly, for a given circRNA c_i and circRNA c_j , the value of $CS(c_i, c_j)$ is $KC(c_i, c_j)$ if $FS(c_i, c_j) = 0$, otherwise $FS(c_i, c_j)$. The integration can be written as follows:

$$CS(c_i, c_j) = \begin{cases} KC(c_i, c_j) & \text{if } FS(c_i, c_j) = 0 \\ FS(c_i, c_j) & \text{otherwise} \end{cases} \quad (7)$$

Similarly, for disease, we combine semantic similarity SS with association profile similarity KD to obtain the disease similarity matrix DS, which can be presented as follows:

$$DS(d_i, d_j) = \begin{cases} KD(d_i, d_j) & \text{if } SS(d_i, d_j) = 0 \\ SS(d_i, d_j) & \text{otherwise} \end{cases} \quad (8)$$

NCPCDA method

In this work, we develop a novel computational method NCPCDA to identify undiscovered circRNA–disease interactions

by using network consistency projection,^{40,41} which is under the assumption that similar circRNAs (or diseases) may well associate with the same disease (or circRNA). Fig. 1 illustrates the implementation framework of NCPCDA, which is implemented based on known circRNA–disease association information and the integrated circRNA similarity and disease similarity.

NCPCDA is composed of disease space projection and circRNA space projection. Specifically, we use disease space projection and circRNA space projection to denote the projection of the disease similarity network and the circRNA similarity network on the disease–circRNA interaction network, respectively. By using vector form, circRNA space projection can be computed by:

$$CSP(i, j) = \frac{CS(i, :) \times Y(:, j)}{|Y(:, j)|} \quad (9)$$

where $CS(i, :)$, which indicates the similarities between circRNA c_i and all circRNAs, is the i -th row vector of matrix CS; $Y(:, j)$, which encodes the correlations between disease d_j and all circRNAs, is the j -th column of matrix Y ; $|Y(:, j)|$ denotes the norm of vector $Y(:, j)$. As a result, the vector projection of $CS(i, :)$ on $Y(:, j)$ can be obtained, represented as $CSP(i, j)$, and we use $CSP \in R^{m \times n}$ to denote the circRNA space projection matrix. According to vector space theory, the projection score $CSP(i, j)$ is positively related to the similarities between circRNA c_i and all circRNAs, to the number of circRNAs associated with disease d_j , while it is negatively related to the angle between $CS(i, :)$ and $Y(:, j)$.

In a similar manner, disease space projection can be presented as follows:

$$DSP(i, j) = \frac{Y(i, :) \times DS(:, j)}{|Y(i, :)|} \quad (10)$$

where $DS(:, j)$ and $Y(i, :)$ are two vectors extracted from the j -th column of disease similarity matrix DS and the i -th row of interaction matrix Y , respectively. As a result, the vector

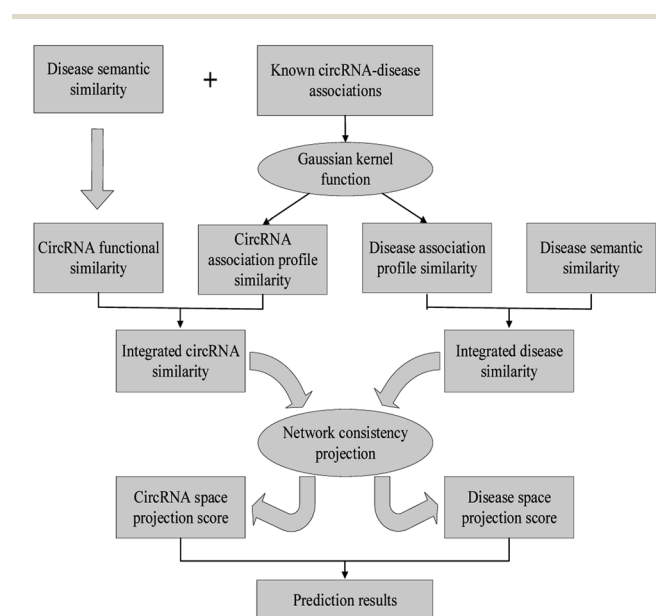


Fig. 1 The overall workflow of the NCPCDA method.



projection of $DS(:,j)$ on $Y(i,:)$ can be obtained, denoted as $DSP(i,j)$, and we use $DSP \in R^{m \times n}$ to represent the disease space projection matrix.

Based on network consistency projection theory, the above two projections scores CSP and DSP could be integrated and normalized by the following formula:

$$NCP(i,j) = \frac{CSP(i,j) + DSP(i,j)}{|CS(i,:)| + |DS(:,j)|} \quad (11)$$

where $NCP(i,j)$ is the final predictive score of circRNA c_i and disease d_j . Since i and j represent any row and column in matrix NCP separately, we can simultaneously obtain the relevance of each circRNA–disease pair.

Results and discussion

Evaluation metrics

We used leave-one-out cross validation and five-fold cross validation to investigate the general prediction performance of NCPCDA. In each leave-one-out cross validation trial, we select a known disease–circRNA association from our dataset in turn as the test sample and suppose this selected pair is unknown in our training samples. All other labeled disease–circRNA pairs and those unobserved pairs are taken as the training set and candidate samples, respectively. For five-fold cross validation, all labeled disease–circRNA pairs are partitioned into five parts at random. One of them is chosen as the test data and the other four parts as training data in turn. In order to eliminate the sampling deviation, we performed ten repetitions of this process. The predictive performance is explained by the receiver operating characteristic (ROC) curve, which draws the false positive rate (FPR) and the true positive rate (TPR) over different score thresholds. Then, we can calculate the area under the curve (AUC) and utilize it as the main metric for prediction accuracy. Given that association profile similarity and circRNA functional similarity depend on known disease–circRNA relationships, they should be recalculated in each fold.

Comparison with other methods

To comparatively illustrate the superiority of NCPCDA, we compare it with PWCDA,¹⁹ KATZHCDA,²⁰ DWNN-RLS,²¹ and CD-LNLP²⁴ as state-of-the-art disease–circRNA interaction prediction approaches. All five prediction methods are evaluated based on the CircR2Disease dataset by adopting leave-one-out cross validation and five-fold cross validation. In Fig. 2, we show the ROC curves of the methods considered here and report their respective AUC values in terms of leave-one-out cross validation. It shows that the ROC curve of NCPCDA is above those of PWCDA, KATZHCDA, DWNN-RLS, and CD-LNLP in most cases, and the AUC score of NCPCDA is up to 0.9541, which is superior to those of the others (PWCDA: 0.9000; KATZHCDA: 0.8672; DWNN-RLS: 0.9180; CD-LNLP: 0.9012). Furthermore, we compared the ROC curves based on five-fold cross validation, which are shown in Fig. 3. The average AUC of NCPCDA reaches 0.9201, while the average AUCs of PWCDA,

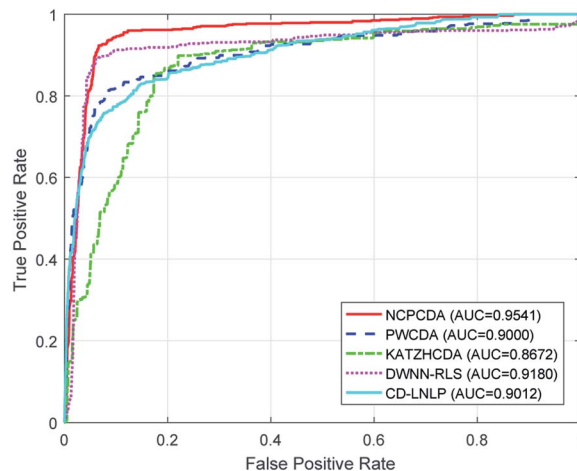


Fig. 2 The ROC curves of different models under leave-one-out cross validation.

KATZHCDA, DWNN-RLS, and CD-LNLP are 0.8900, 0.8632, 0.6503, and 0.7996, respectively. All the above results suggest that NCPCDA provides a great improvement in prioritizing disease–circRNA candidates.

Case studies

In order to examine the ability of NCPCDA to prioritize novel circRNA biomarkers for some cancers, we mainly investigated the following two groups of case studies of lung neoplasms. In the first group, we build the NCPCDA model by using all known disease–circRNA associated pairs from the CircR2Disease dataset and then verify our predictions in another two databases: circRNADisease and Circ2Disease.⁴² Meanwhile, the experimental literature was searched using PubMed for evidence. The top 20 candidate circRNAs for lung cancer are detailed in Table 1, and we confirm four candidates contained in circRNADisease. These four candidate circRNAs,

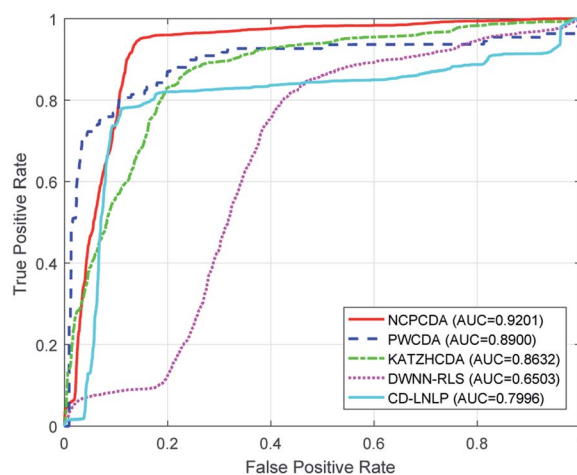


Fig. 3 The ROC curves of different models under five-fold cross validation.



Table 1 The top-20 newly discovered circRNAs for lung cancer predicted by NCPCDA

Rank	circRNAs	Evidence
1	hsa_circ_0007385	PMID: 29372377
2	hsa_circ_0014130	PMID: 29440731
3	hsa_circ_0016760	Unconfirmed
4	hsa_circ_0043256	circRNADisease
5	hsa_circ_0012673	PMID: 29366790
6	hsa_circRNA_404833	PMID: 29241190
7	hsa_circRNA_006411	PMID: 29241190
8	hsa_circRNA_401977	PMID: 29241190
9	hsa_circ_0013958	circRNADisease, Circ2Disease
10	circ-Foxo3/hsa_circ_0006404	PMID: 29620202
11	hsa_circRNA_100782/circHIPK3/hsa_circ_0000284	circRNADisease, Circ2Disease
12	hsa_circ_0023404/circRNA_100876/circ-CER	circRNADisease, Circ2Disease
13	circPRKCI/hsa_circ_0067934	PMID: 29588350
14	hsa_circRNA_100855/hsa_circ_0023028	Unconfirmed
15	hsa_circRNA_104912/hsa_circ_0088442	Unconfirmed
16	hsa_circRNA_103110/hsa_circ_103110/hsa_circ_0004771	Unconfirmed
17	hsa_circ_0001313/circCCDC66	Unconfirmed
18	hsa_circRNA_102049	Unconfirmed
19	hsa_circ_0001649	Unconfirmed
20	CDR1as/ciRS-7/hsa_circ_0001946	PMID: 30841451

hsa_circ_0043256, hsa_circ_0013958, circHIPK3, and circRNA_100876, are all found to be up-regulated in lung cancer cells,^{43–46} three of which are also found in Circ2Disease. Besides, we found literature to support nine predicted circRNAs; see the prediction lists marked as 'PMID' in Table 1. As a result, 13 of 20 predictions are validated to be associated with this disease.

In the second group, by removing all known associated pairs of a certain disease from our training samples, we establish the NCPCDA model and make some necessary predictions for such a disease. The top-ranked predictions for lung cancer are listed in Table 2. As the results show, 4 of the top 20 potential

circRNAs are known to be associated in Circ2Disease. Note that there are only six known circRNAs associated with this cancer in our benchmark dataset. Thus, the recall rate is 66.67% for the top 20 candidates. Moreover, circRNAs circHIPK3 and circZFR are supported by the two aforementioned databases (*i.e.*, circRNADisease and Circ2Disease) or the literature. In addition, we select all known associated pairs of each disease in turn as test samples and carry out predictions. Finally, NCPCDA obtains comparable results with an AUC of 0.9147. These case studies further manifest the applicability of NCPCDA in predicting unobserved disease–circRNA relationships with

Table 2 The top-20 candidate circRNAs for lung cancer predicted by NCPCDA by eliminating all known associated pairs of this disease

Rank	circRNAs	Evidence
1	circMAN2B2/hsa_circRNA_103595	Circ2Disease
2	circRNA_102231	Circ2Disease
3	hsa_circ_0000064	Circ2Disease
4	hsa_circRNA_100782/circHIPK3/hsa_circ_0000284	circRNADisease, Circ2Disease
5	hsa-circRNA 2149	Unconfirmed
6	circular RNA100783/hsa_circ_0008887	Unconfirmed
7	circDLGAP4	Unconfirmed
8	circR-284	Unconfirmed
9	circRNA_104983/hsa_circ_0089974	Unconfirmed
10	circRNA_001059/hsa_circ_0000554	Unconfirmed
11	circRNA_100984/hsa_circ_0002019	Unconfirmed
12	circRNA_100367/hsa_circ_0014879	Unconfirmed
13	circRNA_101877/hsa_circ_0004519	Unconfirmed
14	circRNA_000695/hsa_circ_0001336	Unconfirmed
15	circRNA_101419/hsa_circ_0032832	Unconfirmed
16	circFUT8/hsa_circRNA_101368/hsa_circ_0003028	Unconfirmed
17	circIPO11/hsa_circRNA_103847/hsa_circ_0007915	Unconfirmed
18	hsa_circ_0001313/circCCDC66	Unconfirmed
19	circPVT1/hsa_circ_0001821	Circ2Disease
20	circZFR/hsa_circRNA_103809/hsa_circ_0072088	PMID: 29698681



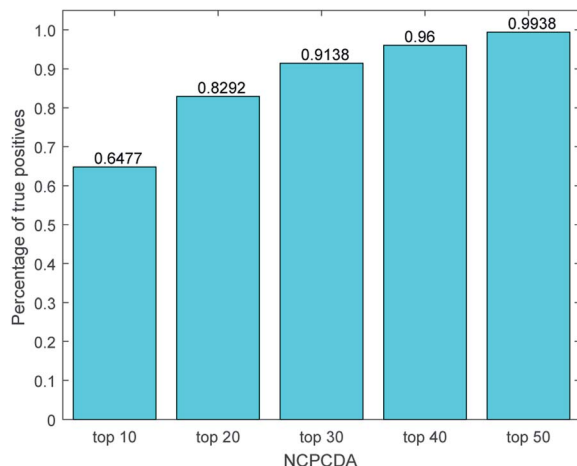


Fig. 4 The percentage of predicted true positives by NCPEDA under different rankings based on the CircR2Disease dataset.

confidence. The predicted circRNAs for all diseases are provided in ESI Table S1.†

We further count the number of true positives under different top portions. As exhibited in Fig. 4, among the 650 true positives, 539 (or 82.92%) interactions are successfully detected in the top 20 predicted pairs. Additionally, we count the results based on the circRNADisease dataset, which collects 332 human disease–circRNA interactions between 40 diseases and 313 circRNAs. As shown in Fig. 5, NCPEDA can detect 260 (or 78.31%) true positives in the top 20 predicted pairs. In order to demonstrate the robustness of our model, five-fold cross validation is also implemented on the circRNADisease dataset. As a result, the average AUC of NCPEDA is up to 0.9367, which is superior to those of three state-of-the-art predictors (KATZHCD: 0.8608; MRLDC: 0.8798; CD-LNLP: 0.9007). This finding illustrates that NCPEDA is effective in identifying true disease–circRNA associations with high rankings.

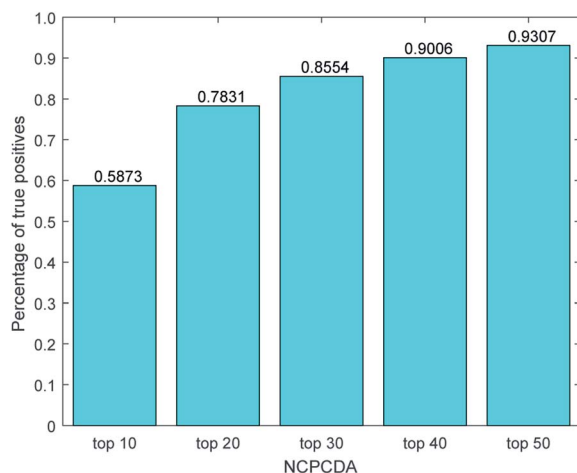


Fig. 5 The percentage of predicted true positives by NCPEDA under different rankings based on the circRNADisease dataset.

Complexity analysis of NCPEDA

The running time of the NCPEDA algorithm is mainly dominated by the computation of the similarity matrix and the network consistency projection score. With regard to similarity data, constructing the circRNA similarity matrix and the disease similarity matrix needs $O(m^2n)$ and $O(n^2m)$, respectively, where m is the size of the circRNA set and n is the size of the disease set in our dataset. For the NCPEDA method, computing the circRNA space projection matrix and the disease space projection matrix also requires $O(m^2n)$ and $O(n^2m)$, respectively. Thus, the computational complexity of the NCPEDA algorithm is $O(m^2n + n^2m)$.

Conclusions

It has been found that circRNAs are associated with various human diseases and have introduced a new dawn in disease diagnosis and prognosis. In this paper, circRNA functional similarity, disease semantic similarity, and association profile similarity are integrated to construct the integrated circRNA similarity and disease similarity. Subsequently, a network consistency projection model is employed to uncover the potential connections between circRNAs and diseases by projecting circRNA space and disease space on the circRNA–disease association network, respectively. We compared NCPEDA with PWEDA, KATZHCD, and DWNN-RLS. The comparative experiments illustrate that our method is powerful in inferring more disease-associated circRNA candidates. Besides, two groups of case studies on lung cancer were implemented, which further showed the good prediction ability of NCPEDA.

The superiorities of NCPEDA over other alternatives are three-fold: (1) it inherits the advantages of a network algorithm, which can fully make use of the topological information of a heterogeneous network; (2) it is a non-parametric algorithm, which can simplify the process of prediction and shorten the prediction time; and (3) it can simultaneously excavate underlying circRNAs for all diseases in our dataset, especially for isolated diseases. Though NCPEDA is simple and effective, it still has several limitations. For starters, the final integrated score is obtained by averaging the circRNA space projection and the disease space projection, which may result in suboptimal predictions. In addition, as the calculation of circRNA similarity is connected with known circRNA–disease links, NCPEDA fails to infer interactions for new circRNAs that do not have any relationship with diseases. Therefore, integrating different types of circRNA data sources, like circRNA sequence data and miRNA–circRNA association data, may aid in expanding our model to predict new circRNAs and improve prediction accuracy.

Conflicts of interest

There are no conflicts to declare.



Acknowledgements

This work was supported by the National Natural Science Foundation of China (Grant No. 61862025, 61873089, 61602283, 11862006, 61861017, and 61862023), the Jiangxi Provincial Natural Science Foundation (Grant No. 20181BAB211016, 2018ACB21032, 20181BAB211013, and 20181BAB202007), the Scientific and Technological Research Project of the Education Department in Jiangxi Province (Grant No. GJJ170383), and the Hunan Provincial Natural Science Foundation (Grant No. 2018JJ2024).

References

- 1 Y. Zhang, X.-O. Zhang, T. Chen, J.-F. Xiang, Q.-F. Yin, Y.-H. Xing, S. Zhu, L. Yang and L.-L. Chen, *Mol. Cell*, 2013, **51**, 792–806.
- 2 C. Cocquerelle, B. Mascrez, D. Hétiuin and B. Bailleul, *FASEB J.*, 1993, **7**, 155–160.
- 3 M. Danan, S. Schwartz, S. Edelheit and R. Sorek, *Nucleic Acids Res.*, 2011, **40**, 3131–3142.
- 4 S. Memczak, M. Jens, A. Elefsinioti, F. Torti, J. Krueger, A. Rybak, L. Maier, S. D. Mackowiak, L. H. Gregersen, M. Munschauer, A. Loewer, U. Ziebold, M. Landthaler, C. Kocks, F. le Noble and N. Rajewsky, *Nature*, 2013, **495**, 333–338.
- 5 L. Chen, C. Huang, X. Wang and G. Shan, *Curr. Genomics*, 2015, **16**, 312–318.
- 6 Q. Chu, X. Zhang, X. Zhu, C. Liu, L. Mao, C. Ye, Q.-H. Zhu and L. Fan, *Mol. Plant*, 2017, **10**, 1126–1128.
- 7 T. B. Hansen, T. I. Jensen, B. H. Clausen, J. B. Bramsen, B. Finsen, C. K. Damgaard and J. Kjems, *Nature*, 2013, **495**, 384–388.
- 8 H.-H. Geng, R. Li, Y.-M. Su, J. Xiao, M. Pan, X.-X. Cai and X.-P. Ji, *PLOS One*, 2016, **11**, e0151753.
- 9 D. Liang and J. E. Wilusz, *Genes Dev.*, 2014, **28**, 2233–2247.
- 10 Z. Zhang, T. Yang and J. Xiao, *EBioMedicine*, 2018, **34**, 267–274.
- 11 Q. Shang, Z. Yang, R. Jia and S. Ge, *Mol. Cancer*, 2019, **18**, 6.
- 12 M. Zhang and Y. Xin, *J. Hematol. Oncol.*, 2018, **11**, 21.
- 13 D. Han, J. Li, H. Wang, X. Su, J. Hou, Y. Gu, C. Qian, Y. Lin, X. Liu, M. Huang, N. Li, W. Zhou, Y. Yu and X. Cao, *Hepatology*, 2017, **66**, 1151–1164.
- 14 B. Chen, W. Wei, X. Huang, X. Xie, Y. Kong, D. Dai, L. Yang, J. Wang, H. Tang and X. Xie, *Theranostics*, 2018, **8**, 4003–4015.
- 15 K.-Y. Hsiao, Y.-C. Lin, S. K. Gupta, N. Chang, L. Yen, H. S. Sun and S.-J. Tsai, *Cancer Res.*, 2017, **77**, 2339–2350.
- 16 J. Chen, Y. Li, Q. Zheng, C. Bao, J. He, B. Chen, D. Lyu, B. Zheng, Y. Xu, Z. Long, Y. Zhou, H. Zhu, Y. Wang, X. He, Y. Shi and S. Huang, *Cancer Lett.*, 2017, **388**, 208–219.
- 17 Z. Zhao, K. Wang, F. Wu, W. Wang, K. Zhang, H. Hu, Y. Liu and T. Jiang, *Cell Death Dis.*, 2018, **9**, 475.
- 18 C. Fan, X. Lei, Z. Fang, Q. Jiang and F.-X. Wu, *Database*, 2018, **2018**, bay044.
- 19 X. Lei, Z. Fang, L. Chen and F.-X. Wu, *Int. J. Mol. Sci.*, 2018, **19**, 3410.
- 20 C. Fan, X. Lei and F.-X. Wu, *Int. J. Biol. Sci.*, 2018, **14**, 1950–1959.
- 21 C. Yan, J. Wang and F.-X. Wu, *BMC Bioinf.*, 2018, **19**, 520.
- 22 Q. Xiao, J. Luo and J. Dai, *IEEE J. Biomed. Health*, 2019, DOI: 10.1109/JBHI.2019.2891779.
- 23 H. Wei and B. Liu, *Briefings Bioinf.*, 2019, DOI: 10.1093/bib/bbz057.
- 24 W. Zhang, C. Yu, X. Wang and F. Liu, *IEEE Access*, 2019, **7**, 83474–83483.
- 25 X. Chen, B. Ren, M. Chen, Q. Wang, L. Zhang and G. Yan, *PLoS Comput. Biol.*, 2016, **12**, e1004975.
- 26 X. Chen and G.-Y. Yan, *Bioinformatics*, 2013, **29**, 2617–2624.
- 27 X. Chen, C. C. Yan, X. Zhang and Z.-H. You, *Briefings Bioinf.*, 2017, **18**, 558–576.
- 28 X. Chen, L. Wang, J. Qu, N.-N. Guan and J.-Q. Li, *Bioinformatics*, 2018, **34**, 4256–4265.
- 29 X. Chen, C.-C. Zhu and J. Yin, *PLoS Comput. Biol.*, 2019, **15**, e1007209.
- 30 X. Chen, C. C. Yan, X. Zhang, X. Zhang, F. Dai, J. Yin and Y. Zhang, *Briefings Bioinf.*, 2016, **17**, 696–712.
- 31 X. Chen, D. Xie, L. Wang, Q. Zhao, Z.-H. You and H. Liu, *Bioinformatics*, 2018, **34**, 3178–3186.
- 32 X. Chen, J. Yin, J. Qu and L. Huang, *PLoS Comput. Biol.*, 2018, **14**, e1006418.
- 33 L. Wang, Z.-H. You, X. Chen, Y.-M. Li, Y.-N. Dong, L.-P. Li and K. Zheng, *PLoS Comput. Biol.*, 2019, **15**, e1006865.
- 34 X. Chen, C. Clarence Yan, C. Luo, W. Ji, Y. Zhang and Q. Dai, *Sci. Rep.*, 2015, **5**, 11338.
- 35 C. Liang, S. Yu and J. Luo, *PLoS Comput. Biol.*, 2019, **15**, e1006931.
- 36 G. Li, J. Luo, Q. Xiao, C. Liang and P. Ding, *J. Biomed. Inf.*, 2018, **82**, 169–177.
- 37 D. Wang, J. Wang, M. Lu, F. Song and Q. Cui, *Bioinformatics*, 2010, **26**, 1644–1650.
- 38 L. M. Schriml, C. Arze, S. Nadendla, Y.-W. W. Chang, M. Mazaitis, V. Felix, G. Feng and W. A. Kibbe, *Nucleic Acids Res.*, 2011, **40**, D940–D946.
- 39 G. Yu, L.-G. Wang, G.-R. Yan and Q.-Y. He, *Bioinformatics*, 2014, **31**, 608–609.
- 40 C. Gu, B. Liao, X. Li and K. Li, *Sci. Rep.*, 2016, **6**, 36054.
- 41 G. Li, J. Luo, C. Liang, Q. Xiao, P. Ding and Y. Zhang, *IEEE Access*, 2019, **7**, 58849–58856.
- 42 D. Yao, L. Zhang, M. Zheng, X. Sun, Y. Lu and P. Liu, *Sci. Rep.*, 2018, **8**, 11018.
- 43 F. Tian, C. T. Yu, W. D. Ye and Q. Wang, *Biochem. Biophys. Res. Commun.*, 2017, **493**, 1260–1266.
- 44 X. Zhu, X. Wang, S. Wei, Y. Chen, Y. Chen, X. Fan, S. Han and G. Wu, *FEBS J.*, 2017, **284**, 2170–2182.
- 45 F. Tian, Y. Wang, Z. Xiao and X. Zhu, *Chin. J. Lung Cancer*, 2017, **20**, 459–467.
- 46 J.-T. Yao, S.-H. Zhao, Q.-P. Liu, M.-Q. Lv, D.-X. Zhou, Z.-J. Liao and K.-J. Nan, *Pathol., Res. Pract.*, 2017, **213**, 453–456.

